International Journal of Soft Computing and Engineering (IJSCE)
ISSN: 2231-2307 (Online), Volume-14 Issue-1, March 2024

An Innovative Approach: Sea Ice Types Classification Using Convolutional Neural Networks with DDDTDWT Filter

Venkata Kondareddy Gajjala, T.J. Naga Lakshmi

Abstract: ***Studying sea ice and its interaction with climate change is crucial due to its significant impact on the environment, society, and global stability. The pressing need to address the underlying reasons for the rapid melting of Arctic and Antarctic sea ice is underscored by its adverse effects on the environment and society. In this proposed study, a Convolutional Neural Network (CNN) is utilized to predict ice types using data from the NSIDC DAAC Advanced Microwave Scanning Radiometer - Earth Observing System Sensor (AMSR-E) collection. This dataset contains parameters such as sea ice types and spans data products from June 2002, obtained from the NASA Data Centre. By employing hand-crafted features as input and a single layer of hidden nodes, the CNN used in this approach generates improved estimates of ice types, outperforming traditional image analysis methods. At each stage, ConvNets utilise diverse filter banks, feature extraction and pooling layers, and fully connected layers with basic activation functions, such as ReLU. This allows the network to build multifaceted hierarchies of features. The sea ice type estimates produced by the CNN are then compared with those obtained from passive microwave brightness temperature data using existing algorithms as well as a proposed CNN algorithm, resulting in an increased classification accuracy of 98.58%. This improvement is particularly notable in the reduction of the error rate, which has been effectively minimized from 3.01% without feature selection to 1.42% with infinite feature selection. When compared to existing algorithms, the CNN demonstrates superior performance. These findings underscore the impact of input patch size, CNN layer count, and input size on the model's performance.***

Keywords: ***Advanced Microwave Scanning Radiometer - Earth Observing System Sensor (AMSR-E), Convolutional Neural Network (CNN).***

I. INTRODUCTION

In the field of operational sea ice analysis, experts use AMSR-E data to create ice charts, which are crucial for providing guidance and support in ice-covered regions. However, manually generating these data analyses is a time-consuming process and can be prone to human errors [1][2].

Manuscript received on 07 February 2024 | Revised Manuscript received on 06 March 2024 | Manuscript Accepted on 15 March 2024 | Manuscript published on 30 March 2024.

*Correspondence Author(s)
Dr. Venkata Kondareddy Gajjala*, Department of Computer Science and Engineering, N.B.K.R. Institute of Science and Technology, Tirupati, India. E-mail ID: gvkondareddy@gmail.com ORCID ID: 0000-0002-3232-4451
Dr. T.J. Naga Lakshmi, Professor, Department of Electronics and Communication Engineering, Saveetha Institute of Medical and Technical Sciences, Chennai, India. E-mail ID: nagalakshmitj.sse@saveetha.com ORCID ID: 0000-0003-2690-8642

With new satellite missions such as AMSR-E and the European Sentinel mission, we anticipate a significant increase in the volume of satellite imagery. The increasing volume of data poses a challenge in efficiently analyzing and processing imagery. Previous studies have explored automated methods for extracting valuable information from AMSR-E imagery. These studies have utilised specific features tailored for particular tasks, such as HH autocorrelation, cross-polarisation ratio, and scaled polarisation difference, for estimating sea ice concentration. Over its operational lifespan, AMSR-E data have significantly enhanced our understanding of the seasonal evolution of sea ice, providing essential insights into the dynamic changes that occur over time. AMSR-E, operating as a passive microwave radiometer, is unaffected by sunlight and specific channels are not impacted by clouds, allowing data collection even in cloudy conditions. Various techniques, such as grey-level co-occurrence matrix features, Gabor filters, and Markov random fields, have been successfully used to classify AMSR-E imagery into different ice types and ice/water conditions. Generating a robust set of engineered features for automatic information extraction from Synthetic Aperture Radar (SAR) imagery poses a significant challenge. It needs to be adaptable across diverse geographic regions, seasons, and imaging geometries. To comprehensively capture a wide range of ice conditions, it may be necessary to tailor features specific to various locations or seasonal variations. For example, creating a comprehensive database containing HH and HV backscatter values calculated on a region-specific basis, considering factors such as incidence angles and wind speeds, could prove to be invaluable. Analysts derive sea ice concentration estimates from AMSR-E images, relying heavily on their nuanced understanding of local sea ice conditions and adept interpretation of visual cues within the pictures. This complex process involves examining diverse characteristics of AMSR-E images across different scales. Emulating the visual method's capability to synthesize information from various scales and incorporate past knowledge is necessary to carry out this task effectively. CNN has a solid reputation for its ability to extract features from images, excelling precisely at considering information across various scales.

In the current research, a CNN is employed to classify ice types based on the acquired AMSR-E imagery. This innovative approach not only promises efficiency and accuracy but also aligns with the evolving technological landscape in sea ice analysis.

II. BACKGROUND WORK

Consider using image feature learning from AMSR-E imagery for ice concentration estimation, which expands upon the feature learning methods used in previous research. This approach has the potential to analyze complex datasets effectively. Deep learning, a type of feature learning, can autonomously interpret complex data visuals at high abstraction levels. In the field of image recognition, deep CNNs are widely used due to their efficiency in modelling local image structures at different scales [12][13][14][15].

However, there has been limited research on using CNNs to extract features from satellite imagery. Training CNN models requires a large volume of high-quality training data, which can be expensive and impractical to obtain, especially for tasks such as ice concentration due to the extensive geographical coverage and diverse surface conditions. This challenge is particularly evident in functions related to ice concentration, as algorithms designed for estimating ice types from passive microwave data may exhibit biases, especially in areas with thin ice and low ice concentration levels [3][4][5]. The assessments provided by analysts are generally considered the most reliable and accurate source of information on ice concentration. Therefore, the extensive image analysis database available at the NASA Image Data Store can be utilized to explore the application of a CNN for estimating ice types from AMSR-E imagery.

III. PROPOSED WORK ARCHITECTURE-CNN WITH DDDTDWT FILTER

In this study, the Double Density Dual-Tree Discrete Wavelet Transformation (DDDTDWT) is used as a technique to remove noise from images of different types of ice. We also apply Grey Level Co-Occurrence Matrices (GLCM) for feature extraction. We select suitable features such as contrast, dissimilarity, energy, entropy, homogeneity, correlation, and variance for classification [6-11].

During the process, oriented wavelets are generated using the dual-tree double-density 2-D transformation, and the 2-D input image undergoes a type-tree discrete wavelet transformation. In this transformation, use "fdf" for the first level and "df" for subsequent levels as the analysis filters. The coefficients resulting from the DDDTDWT image filtering are organised. A structured version of the Grey-Level Co-occurrence Matrix (GLCM) is used to derive feature values for each ice type, which are then organised into a matrix.

As part of the DDDTDWT approach, the results are provided to the convolutional neural network algorithm, as shown in Figure 1.

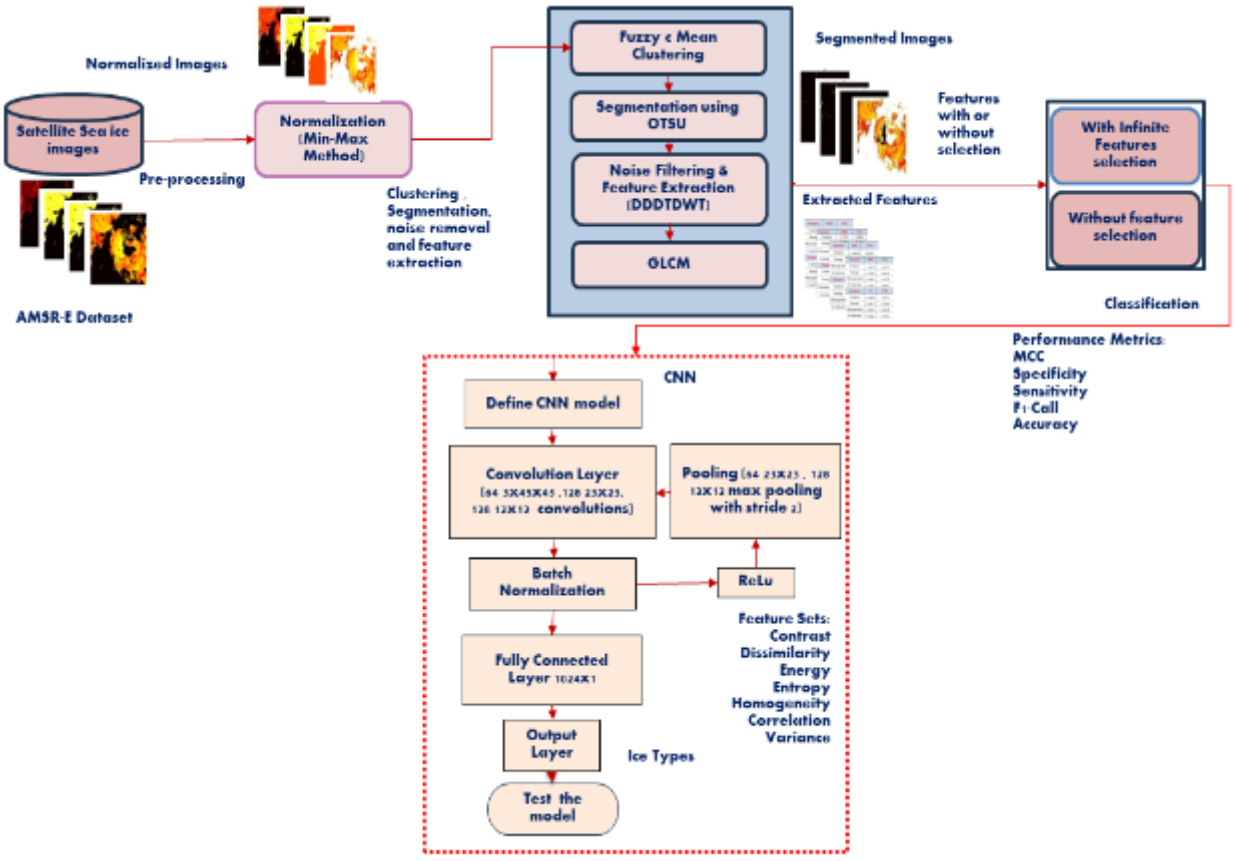

Figure 1. Proposed Work Architecture-CNN with DDDTDWT Filter

Specifically, the AMSR-E/Aqua Daily L3 12.5 km Sea Ice Concentration, & Snow Depth Polar Grids V003 Level-3 gridded product (AE_SI12) includes brightness temperatures ranging from 18.7 to 89.0 GHz, sea ice concentration, and snow depth over sea ice in dual-pol (HH and HV) Polarizations. These comprehensive datasets provide a thorough understanding of sea ice conditions in the study area over the specified time frame.

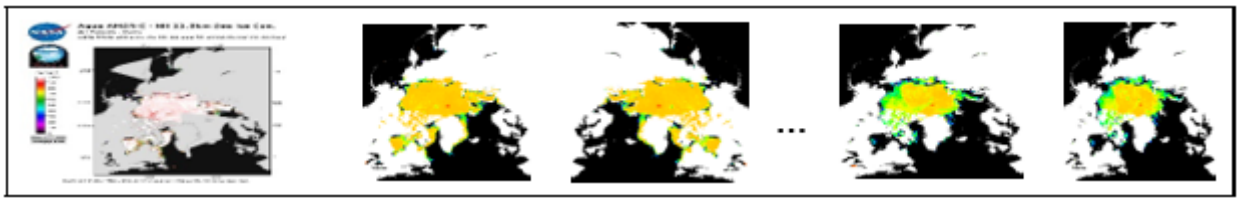

Figure 2a) Study Area , Figure 2b) The dataset for the AMSR-E Level 3 Standard Sea Ice Products

A. Dataset: AMSR-E Imagery

The study area, as illustrated in Figures 2(a) and 2(b), encompasses data spanning a decade from July 2, 2012, to December 14, 2022, utilising AMSR-E imagery. Throughout the study duration, Sea ice products with AMSR-E Level 3 standard were supplied by the National Snow and Ice Data Centre (NSIDC). These products comprise sea ice concentration, generated using the NT2 algorithm, sea ice temperature, and snow depth on sea ice produced from the AMSR-E algorithm [16].

B. AMSR-E Images Pre-processing

To optimise the management of data volume and reduce image speckle noise, a crucial step is taken with all AMSR-E images, which involves subjecting them to an 8 × 8 block averaging process. Neural networks become more efficient when operating at this reduced scale, as it requires a smaller spatial context window. This approach gains favour due to the relatively limited number of available training samples. The sub-sampled images maintain a pixel spacing of one kilometre, with pixel values ranging from 0 to 255. Enhancing CNN performance typically involves employing input normalisation. In this investigation, a normalisation procedure is applied to the pixel values in the dual-polarised AMSR-E images. This consists of computing the mean and standard deviation of pixel values across the entire dataset for each channel. Subsequently, these calculated means are subtracted from each pixel value, followed by division by the respective standard deviation.

When selecting training sample patches in proximity to the land, challenges arise as the CNN may encounter confusion. Land pixels have the potential to misrepresent nearby water areas, creating an illusion of ice where there is none. The impact of this issue is contingent on the size of the training patches. In this instance, 45 by 45 pixel patches are used, equivalent to approximately 2 kilometres by 2 kilometres on the ground. A straightforward removal of land pixels and setting them to 0 could introduce misinterpretations. Instead of the straightforward removal of land pixels, a land mask is applied to the AMSR images, replacing land pixels with those resembling either ice or water. This strategic move reduces land interference, and although it may lead to reliance on nearby ice or water pixels for ice concentration determination, tests demonstrate that the land mirroring method effectively mitigates the impact of land on ice concentration and extent estimates. Currently, alternative methods for masking land pixels remain unexplored.

In addition, the incidence angle of each pixel in the AMSR image is carefully computed to understand the surface interaction of the signal generated by the radar. These angle values are then transformed into images, ensuring a range of values similar to the AMSR images themselves. Each extracted patch, coupled with the ice concentration and extent located at the patch centre from image analysis, serves as a single sample used to train the CNN. In cases where patches exhibit a boundary shape, they are labelled based on the shape of the central pixel, although using a label that describes the ice concentration as a mix of both shapes might offer greater accuracy. These challenges serve as the basis for further exploration in future research endeavours.

C. Overview and Configuration of the CNN

A Convolutional Neural Network (CNN) functions as a learning structure with distinct components, each undergoing three crucial steps: convolutional filtering, non-linear transformation, and pooling layers. Typically, a CNN is composed of several of these parts, each of which learns different features of an image. Subsequently, additional layers interconnect these learned features. In this context, a CNN is designed with three filtering layers and two connecting layers, as outlined. The detailed architecture of this CNN is illustrated in Figure 1 [17][18].

Within the convolutional layers, K convolution filters of size (C_xC_y, C_z), labelled as C^k, convolve the input matrix (width of S_x pixels, height of $S_y$pixels, and the number of channels designated as S_z) representing a patch recovered from the AMSR image [19][20][21][22]. The image patch is subjected to each filter with a stride indicated by P. The outcome of this convolutional operation results in K feature maps, denoted as h^k, each having dimensions $M_x$and M_y as outlined in Equation (1) [23][24][25].

$$h^k = (C^k * x) + b \text{ in which , k} = 1,2 \ldots \text{K} \quad (1)$$

$$M_x = \frac{S_x - C_x}{P} + 1$$

$$M_y = \frac{S_y - C_y}{P} + 1$$

In this context, the symbol $(*)$ is utilized to illustrate the convolution process. The size of the feature maps ($M_x \times M_y$) is specified when considering padding in images. Each convolutional layer incorporates filters of varying sizes and quantities, learning the values of these filter weights and a parameter known as bias from the training data.

Every element in the feature maps is subjected to the activation function after the convolution. Here, the Rectified Linear Unit (ReLu) activation function is employed, surpassing the older sigmoid function as it accelerates the learning process and yields superior features.

Post the non-linear transformation, the subsequent step is sub-sampling or pooling.

Max pooling is adopted due to its simplicity and effective performance (LeCun, 2010). Max pooling outputs the maximum value within each pooling window. For instance, with a pooling window size and step size both set to 2, a max-pooling layer produces the maximum value within every non-overlapping 2x2 window of its input. The convolutional layers are followed by fully connected layers, which serve as classification modules that utilise features extracted from earlier stages. Each neuron in a fully connected layer is connected to all neurons of its input layer. The initial fully connected layer takes a stack of feature maps (h^k) as inputs. These feature maps, arranged in a flat, linear format, are transformed into the output space using a weight matrix, W, and a bias, b. Subsequently, the function f is employed to generate the output [26-36].

D. Learning and Assessments

The network is configured for predicting ice types from AMSR-E image patches. Utilising the loss function, discrepancies between the CNN output and ice types identified through image analysis are penalised. Following each training session, the loss function is evaluated by computing the loss using the current model on the validation dataset. Commonly used in regression tasks, the loss function quantifies the squared disparity between predicted and actual values, with the objective of minimizing this difference. Here, the training employs backpropagation with mini-batch stochastic gradient descent (SGD), which leverages the derivatives of the loss function. These variations are backpropagated through each pixel in the predictions, updating network elements based on the variations of the loss to the parameters over each mini-batch. Sequential adjustments to the training parameters are implemented, following an epoch-based training approach, where each epoch iterates through all training samples once. Every 20,000 mini-batches, the learning rate is reduced by a factor of 10 to improve training efficiency. Training concludes when the loss function's score exhibits minimal change (less than 0.001) for 20 consecutive epochs, preventing early convergence, a common occurrence. A supplemental method called dropout is used to lessen overfitting. A dropout layer stochastically sets neuron outputs in a layer to zero with a predetermined probability. In this case, a dropout layer with a dropout rate of 0.5 is utilized, randomly selecting half of the neurons, forcing the network to acquire more representative features. For experimentation, 500 scenes are randomly divided into 400 learning images and the remainder for assessment images. Post-training the CNN model, it is applied to estimate ice types for each pixel location in the target AMSR-E images. The CNN model, employing a stride of 1 on input images, advances the input window one pixel at a time during forward propagation.

IV. IMPLEMENTATION AND UTILIZATION

Utilised tools in Python, including TensorFlow, GeoPandas, Basemap, and PyTorch. TensorFlow, a comprehensive framework, provides extensive tools and resources for constructing and training neural networks. Complementary to the pandas library, GeoPandas broadens its capabilities to handle geospatial data effectively. Basemap, a toolkit for Matplotlib, facilitates the creation of static, interactive, and publication-quality maps, proving useful for various mapping and visualization tasks. Renowned for its flexibility and dynamic computation graph, PyTorch is employed. In the Python environment, the implementation of AMSR-E image pre-processing and patching leverages the capabilities of these tools. TensorFlow and PyTorch contribute to the construction and training of neural networks, while GeoPandas and Basemap enhance the handling and visualization of geospatial data, offering a robust framework for comprehensive AMSR-E image analysis.

A. Ice Types and Their Features

Feature selection is accomplished using the infinite feature selection method. Table 9.1 displays the features of various ice types, including multi-year ice (MYI), first-year ice (FYI), young ice (YI), and open water (OW), with and without selection.

In this context, MYI refers to ice that has endured at least one melt season and is typically 2 to 4 meters thick. FYI, ice is thicker than 30 centimetres but has not experienced a summer melt season. YI represents ice formed during the current winter season and is less than one year old. OW designates areas without ice coverage.

For C-NN, specific features are identified, such as contrast, dissimilarity, energy, homogeneity, correlation, and variance. Contrast measures intensity differences between neighbouring pixels, which helps distinguish high and low ice concentrations or extents. Dissimilarity, a measure of intensity differences, also aids in distinguishing ice concentrations or extents. Energy, the sum of squared pixel values, measures the overall brightness of ice characteristics in an image. Homogeneity, reflecting pixel similarity, helps identify uniform ice areas. Correlation, which indicates linear relationships, can reveal patterns in ice characteristics. Variance, which measures the spread of pixel values, identifies areas of high or low ice concentration. These feature values are then utilised in the next step to select the desired features.

B. CNN Classification with Infinite Feature Selection and Without Feature Selection by Using DDDTDWT Filter

Now, this applies to features derived from the outcomes of the noisy single and double filter using DDDTDWT with the GLCM transformation technique, both with and without feature selection. With a single filter and double filters, we have checked with a selected number of features. After the results, changes have been observed with either a single filter or a double filter. A limited number of features, including contrast, energy, correlation, and homogeneity, are chosen with an infinite feature selection method for classification.

In the context of CNN, features such as contrast, energy, homogeneity, correlation, dissimilarity, entropy, and variance have been selected using the Infinite Feature selection method. Here, dissimilarity is a measure of the difference in intensity between neighbouring pixels in an array element, used to distinguish between areas of high and low ice concentration or ice extent. Entropy is a measure of the randomness or disorder in an array of elements, called feature values, which identify areas of mixed ice types or concentrations, typically characterised by higher entropy values.

Retrieval Number: 100.1/ijsce.B809913020724
DOI: 10.35940/ijsce.B8099.14010324
Journal Website: www.ijsce.org

Published By:
Blue Eyes Intelligence Engineering
and Sciences Publication (BEIESP)

Variance is a measure of the spread of pixel values in an array element to identify areas of high or low ice concentration or ice extent. These feature values are subsequently used in the next step to select the desired features, as illustrated in Table 1.

Table 1. Features of Ice Types Derived After Filtering by Using DDDTDWT and GLCM with a 4-Band Single Image

Features	MYI	FYI	YI	OW
Contrast	2.0112	2.853	0.2881	2.0269
Dissimilarity	0.3184	0.4298	0.0427	0.3122
Energy	0.8066	0.7625	0.9451	0.4485
Entropy	0.5053	0.6071	0.1542	0.9806
Homogeneity	0.9554	0.9395	0.9943	0.9558
Correlation	0.6780	0.6268	0.8772	0.9167
Variance	5.5241	6.3561	2.5119	32.3216

In the Table 1, Contrast, and Dissimilarity is more in FYI, and less in YI; Energy is more in YI, and less in OW; Entropy is more in OW, and less in YI; Homogeneity is more in YI, and less in FYI; Correlation is more in OW, and less in FYI; Variance is more in OW and less in YI.

C. Selection of Features

Here, selected features include contrast, energy, homogeneity, and correlation. The selected features are determined using an infinite feature selection algorithm based on the mean and intensity values of the features shown in Table 2.

Table 2. Features of Ice Types by Using Infinite Feature Selection

Features	MYI	FYI	YI	OW
Contrast	2.0112	2.853	0.2881	2.0269
Energy	0.8066	0.7625	0.9451	0.4485
Homogeneity	0.9554	0.9395	0.9943	0.9558
Correlation	0.6780	0.6268	0.8772	0.9167

NOTE: MYI-Multi Year Ice, FYI-First Year Ice, YI-Young Ice, OW-Open Water

D. Performance Metrics for all Ice Types with Infinite Feature Selection and Without Feature Selection

Here, Table 3 displays the results obtained using overall accuracy, error rate, and various metrics like Matthews's correlation coefficient (MCC), sensitivity, specificity, and F1-score. Matthews's correlation coefficient (MCC) provides a score between -1 and +1, taking into account true positives, true negatives, false positives, and false negatives. A score of +1 signifies a perfect prediction, 0 indicates a random prediction, and -1 represents the opposite.

Sensitivity, also known as the actual positive rate (TPR), measures the proportion of correctly identified actual positives among all actual positives. In the context of sea ice, it assesses a classification model's ability to identify different ice types accurately. Specificity, or the actual negative rate (TNR), assesses the proportion of correctly identified actual negatives. In the sea ice scenario, it assesses the classification model's ability to identify areas without specific ice types accurately. F1-Score, the harmonic mean of precision and recall, considers false positives and false negatives. In the context of sea ice, it evaluates the overall accuracy of a classification model in identifying various ice types. Accuracy, the ratio of correctly classified samples to the total number of samples, measures the overall performance of a classification model. In the sea ice scenario, it reflects the model's ability to identify different areas with specific ice types accurately.

Table 3. Performance Metrics of Ice Types with Infinite Feature Selection and Without Feature Selection by Using DDDTDWT and GLCM

Ice Type	Strategy	Mcc	Sensi	Speci	F_1-Score	Acc	Error
MYI	WITH-FS	1	0.999	0.986	0.987	0.993	0.007
	WITH OUT-FS	0.995	0.986	0.986	0.978	0.986	0.013
FYI	WITH-FS	0.998	0.999	0.989	0.979	0.991	0.009
	WITH OUT-FS	0.975	0.972	0.969	0.934	0.962	0.038
YI	WITH-FS	1	0.993	0.945	0.959	0.974	0.026
	WITH OUT-FS	0.989	0.978	0.928	0.989	0.971	0.029
OW	WITH-FS	0.997	0.978	0.976	0.99	0.985	0.015
	WITH OUT-FS	0.925	0.962	0.963	0.989	0.959	0.04

V. RESULTS EXAMINATION

In this context, one critical parameter has been examined, namely sea ice type. This parameter serves as an essential tool in the exploration of sea ice dynamics, climate change, and their profound impacts on both polar and global environments. Extensively employed by researchers and scientists, these parameters provide valuable insights into the state and behavior of sea ice across diverse regions and seasons. Their thorough examination contributes to a deeper understanding of the intricate dynamics governing sea ice, facilitating comprehensive analyses of its responses to environmental changes on a regional and global scale.

A. CNN Classification with Infinite Feature Selection and Without Features by using DDDTDWT Filter

This approach enables the identification of relevant attributes for ice types. Ultimately, the generated performance measures encompass various metrics for each class type, including overall accuracy, MCC, sensitivity, specificity, and F1-score, all achieved through the utilisation of the classification methodology shown in Table 4.

This methodology facilitates the identification of distinct ice types, including Multi-Year Ice (MYI), First-Year Ice (FYI), Young Ice (YI), and Open Water (OW). Multi-Year Ice (MYI) refers to ice that has endured at least one melt season and is typically 2 to 4 meters (6.6 to 13.1 feet) thick, thickening as additional ice accumulates on its underside. First-Year Ice (FYI) is thicker than 30 centimetres (11.8 inches) but has not survived a summer melt season. Young Ice (YI) forms during the current winter season and is less than one year old, while Open Water (OW) remains uncovered by ice.

Table 4. CNN Classification Performance Metrics of Ice Types with Infinite Feature Selection and Without Feature Selection by Using DDDTDWT

Strategy	Mcc	Sensi	Speci	F1 -Score	Acc	Error Rate
With FS	0.9987	0.9922	0.974	0.9787	0.9858	0.0142
Without FS	0.9713	0.9745	0.9615	0.9725	0.9698	0.0301

Note: FS- Feature Selection, SENSI-Sensitivity, SPECI-Specificity, ACC-Accuracy

Ultimately, the evaluation encompasses diverse metrics for each ice type, including overall accuracy, Matthews Correlation Coefficient (MCC), sensitivity, specificity, and F1-score, as determined by the classification methodology outlined in Table 4. As shown in Table 4, The Performance metrics of the CNN with infinite feature selection and a remarkable accuracy rate of 98.58% are noted across various ice types, as depicted in Figure 3. The error rate was 1.42%. When comparing results with infinite feature selection and without feature selection, utilizing the de-noising filter DDDTCWT and GLCM transformation technique, the CNN classifier demonstrated improved accuracy by 0.48 per cent with M-SVM [35].

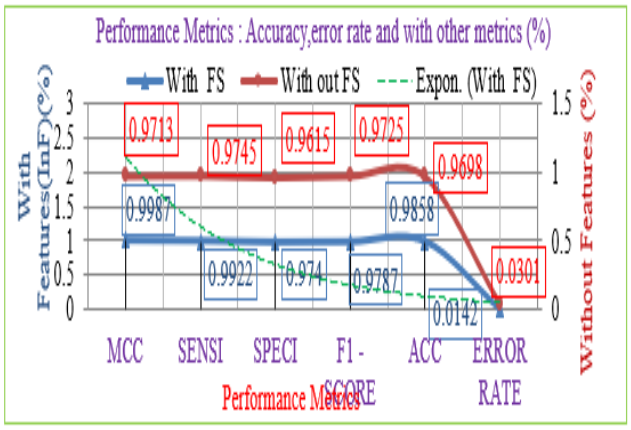

Figure 3. Illustrates the Evaluation Outcomes with Infinite Feature Selection and Without Feature Selection by using DDDTDWT Filter. Note: FS- Feature Selection, SENSI-Sensitivity, SPECI-Specificity, ACC-Accuracy

In a summary, accuracy rate of 98.58 percent was observed across ice types, accompanied, as demonstrated in Figure 3 with infinite feature selection by an error rate of 1.42%, and without feature selection by an error rate of 3.01 percent through the utilization of the de-noising filter DDDTDWT and GLCM transformation technique, the accuracy of the CNN classifier is enhanced 1.59 percent. Furthermore, there is a significant improvement in other performance parameters, including MCC at 99.87% sensitivity and 99.22% specificity, and F_1-score at 97.87% with infinite feature selection.

B. Comparisons Between Proposed CNN and Existing Algorithms with Infinite Feature Selection and Without Feature Selection Using DDDTDWT Filter

The comparison of CNN with existing algorithms, including infinite feature selection and without feature selection by using DDDTDWT Filter. Note: FS- Feature selection shown in Table 5.

Table 5. Comparison of Proposed Method on Accuracy and Error Rate with Existing Algorithms with Infinite Feature Selection by using DDDTDWT

S. No	Method	Accuracy	Error Rate
1	Proposed a CNN by using DDDTDWT	98.58%	1.42%
2	Wang, Lei, et. al.[31] by using RF	96.20%	4.80 %
3	Wang, Lei, et. al. [32] by using NN	89.10%	10.80%
4	Giorgio Roffo et. al. by using Feature Selection	94.60%	5.40%

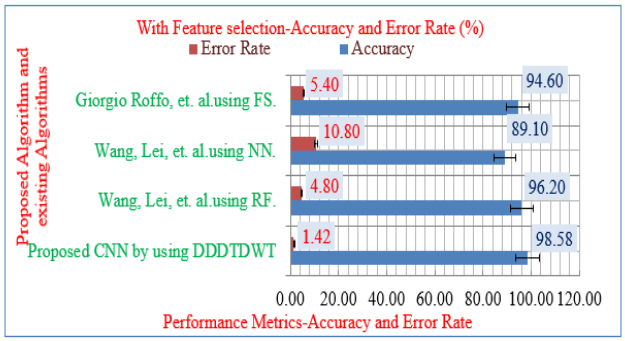

Figure 4. Comparison of all Proposed Methods on Accuracy and Error Rate with Existing Algorithms with Infinite Feature Selection by Using DDDTDWT Filter

By Chai, Hum Y. et al., Giorgio Roffo et al., and Wang et al., various approaches have been employed to enhance classification accuracy. For instance, the utilisation of GLCM has yielded improvements, and feature selection techniques have also been applied. Furthermore, the combination of RF and NN has been explored to achieve favourable outcomes, notably through the implementation of the C-NN algorithm, which resulted in a 98.58% enhancement in classification accuracy, as depicted in the graphical representation presented in Figure 4. This improvement is especially evident in the reduction of the error rate, which has been effectively 1.42% through the CNN with infinite feature selection using DDDTDWT.

Retrieval Number: 100.1/ijsce.B809913020724
DOI: 10.35940/ijsce.B8099.14010324
Journal Website: www.ijsce.org

Published By:
Blue Eyes Intelligence Engineering and Sciences Publication (BEIESP)

Table 6. Comparison of all Proposed Methods on Accuracy and Error Rate with Existing Algorithms Without Feature Selection by Using DDDTDWT

S. No	Method	Accuracy	Error Rate
1	Proposed a CNN by using DDDTDWT	96.98%	3.01%
2	Wang, Lei, et. al. [31] by using RF.	96.20%	4.80 %
3	Wang, Lei, et al. [31] used NN.	89.10%	10.80%
4	Giorgio Roffo et. al. by using FS.	94.60%	5.40%

By Chai, Hum Y. et al., Giorgio Roffo et al., and Wang et al., various approaches have been employed to enhance the classification accuracy, as shown in Table 6. For instance, the utilisation of GLCM has yielded improvements, and feature selection techniques have also been applied.

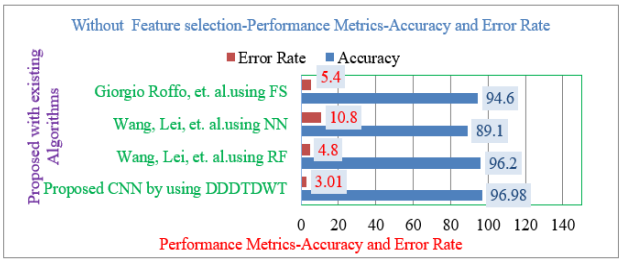

Figure 5. Comparison of All Proposed Methods on Accuracy and Error rate with existing algorithms Without Feature Selection by Using DDDTDWT Filter

Furthermore, the combination of RF and NN has been explored to achieve favourable outcomes, notably through the implementation of the C-NN algorithm, which resulted in a 96.98% enhancement in classification accuracy, as depicted in the graphical representation presented in Figure 5. This improvement is especially evident in the reduction of the error rate, which has been effectively 3.01% through the CNN without feature selection using DDDTDWT.

VI. CONCLUSIONS AND FUTURE ENHANCEMENTS

In the exploration of ice types, an innovative system was developed to identify various ice types within a sea ice block by analysing satellite sea ice images. In an exploration with infinite feature selection using DDDTDWT, the utilisation of GLCM has yielded improvements. Furthermore, the combination of RF and NN has been explored to achieve favourable outcomes. Notably, through the implementation of the CNN algorithm, a 98.58% enhancement in classification accuracy was achieved. This improvement is especially evident in the reduction of the error rate, which has been effectively minimised from 3.01% (without feature selection) to 1.42% through the use of the CNN algorithm.

DECLARATION STATEMENT

Funding	No, I did not receive.
Conflicts of Interest	No conflicts of interest to the best of our knowledge.
Ethical Approval and Consent to Participate	No, the article does not require ethical approval or consent to participate, as it presents evidence that is not subject to interpretation.
Availability of Data and Materials	Not relevant.
Authors Contributions	All authors have equal participation in this article.

REFERENCES

1. Carrieres, T.; Greenan, B.; Prinsenberg, S.; Peterson, I.," Comparison of Canadian daily ice charts with surface observations off Newfoundland", winter 1992. Atmos. Ocean 1996, 34, 207–226, Oct 1996. https://doi.org/10.1080/07055900.1996.9649563
2. Masahiro Kazumori, "Impact Study of AMSR-E Radiances in the NCEP Global Data Assimilation System", Page (s): 541–559, 2008. https://doi.org/10.1175/2007MWR2147.1
3. J. Rohrs and L. Kaleschke An algorithm to detect sea ice leads by using AMSR-E passive microwave imagery ".Articles European Geoscience union Volume 6, issue 2 TC, 6, 343–352, 2012. https://doi.org/10.5194/tc-6-343-2012
4. Ayushman Ramola, Study of statistical methods for texture analysis and their modern evolutions", 2022.
5. Clausi, D.A., et al.," Comparison and fusion of co-occurrence, Gabor, and MRF texture features for classification of SAR sea ice imagery. Atmos. Ocean 39, 183–194, 2001. https://doi.org/10.1080/07055900.2001.9649675
6. Pogson, L et al.," A collection of empirically derived characteristic values from SAR across a year of sea ice environments for use in data assimilation", Mon. Weather Review Press, 2016. https://doi.org/10.1175/MWR-D-16-0110.1
7. Buehner, M.; Caya, A.; Pogson, L.; Carrieres, T.; Pestieau, "PA new Environment Canada regional ice analysis system".Atmos.Ocean, *51*,18–34, 2013. https://doi.org/10.1080/07055900.2012.747171
8. Drusch, M. et al., "Sea ice concentration analyses for the Baltic Sea and their impact on numerical weather prediction", J.Appl.Meteorol. Climatol *45*,982 994, 2006. https://doi.org/10.1175/JAM2376.1
9. LeCun, Y.; Bengio, J.; Hinton, G. Deep Learning. *Nature*, 521,436–444, 2015. https://doi.org/10.1038/nature14539
10. Wang, L.; Scott, K.A.; Xu, L.; Clausi, D.A.," Sea Ice Concentration Estimation During Melt From Dual-Pol SAR Scenes Using Deep Convolutional Neural Networks: A Case Study", IEEE Trans. Geosci. Remote Sens. 2016, 54, 4524–4533. https://doi.org/10.1109/TGRS.2016.2543660
11. Ivanova, N.; Tonboe, R.; Pedersen," L.T.SICCI Product Validation and Algorithm Selection Report (PVASR)-Sea Ice Concentration", Technical Report; European Space Agency: Paris, France, 2013.
12. Najafabadi, M.M.; Villanustre, F.; Khoshgoftaar, T.M.; Seliya, N.; Wald, R.; E., "Deep learning applications and challenges in big data analytics" Big Data, 2, 2015. https://doi.org/10.1186/s40537-014-0007-7
13. Mnih, V.; Hinton, G.- Learning to detect roads in high-resolution aerial images. In Computer Vision-ECCV", Springer: Berlin/Heidelberg, Germany, pp.210-223, 2010. https://doi.org/10.1007/978-3-642-15567-3_16
14. Chen, X.; Xiang, S.; Liu, C.L.; Pan, C.H.," Vehicle Detection in Satellite Images by Hybrid Deep Convolutional Neural Networks". IEEE Geosci. Remote Sens. Lett. 11, 1797-1801, 2014. https://doi.org/10.1109/LGRS.2014.2309695
15. Maggiori, E.; Tarabalka, Y.; Charpiat, G.; Alliez, P. Fully convolutional neural networks for remote sensing image classification. In Proceedings of the 2016 IEEE Geoscience and Remote Sensing Symposium, Beijing, China, 10-15,2016. https://doi.org/10.1109/IGARSS.2016.7730322
16. Karvonen, J.; Vainio, J.; Marnela, M.; Eriksson, P.; Niskanen, T.)A comparison between high-resolution EO-based and ice analyst-assigned sea ice concentrations. J. Sel. Top. Appl. Earth Obs. Remote Sens 8, 1799–1807, 2015. https://doi.org/10.1109/JSTARS.2015.2426414
17. Hastie, T.; Tibshirani, R.; Friedman, J. The Elements of Statistical Learning; Springer: Berlin/Heidelberg, Germany Volume 2, 2009. https://doi.org/10.1007/978-0-387-84858-7
18. Bishop, C.M. Pattern Recognition and Machine Learning; Springer: Berlin/Heidelberg, Germany, 2006.
19. Le Cun, Y.; Kavukcuoglu, K.; Farabet, C.," Convolutional networks and applications in vision. In Proceedings of IEEE International Symposium on Circuits and Systems (ISCAS), Paris, France, 30 May–2 June 2010; pp. 253–256, 2010. https://doi.org/10.1109/ISCAS.2010.5537907
20. https://github.com/tensorflow/tensorflow
21. https://en.wikipedia.org/wiki/PyTorch
22. https://en.wikipedia.org/wiki/Measurement_of_sea_ice
23. Krizhevsky, A.; Sutskever, I.; Hinton, G.E. ImageNet classification with deep convolutional neural networks. In Proceedings of the 25th International Conference on

Neural Information Processing Systems, Lake Tahoe, NV, USA, 3-6; pp. 1097-1105, December 2012.
24. Karpathy, A.; Toderici, G.; Shetty, S.; Leung, T.; Sukthankar, R.; Fei-Fei, L. Large-scale video classification with convolutional neural networks. In Proceedings of the 2014 IEEE Conference on Computer Vision and Pattern Recognition, Columbus, OH, USA, pp. 1725-1732,2014. https://doi.org/10.1109/CVPR.2014.223
25. Chen, L.C.; Papandreou, G.; Kokkinos, I.; Murphy, K.; Yuille, A.L.
26. Semantic image segmentation with deep convolutional nets and fully connected CRFs. arXiv, arXiv:1412.7062, 2016. LeCun, Y.; Bottou, L.; Orr, G.; Müller, K. Efficient backprop. In Neural Networks: Tricks of the Trade; Springer: Berlin/Heidelberg, Germany, 2012
27. Prechelt, L Early stopping-but when? In Neural Networks: Tricks of the Trade; Springer: Berlin/Heidelberg, Germany, pp. 53-67, 2012. https://doi.org/10.1007/978-3-642-35289-8_5
28. Hinton, G.E.; Srivastava, N.; Krizhevsky, A.; Sutskever, I.; Salakhutdinov, R.R. Improving neural networks by preventing co-adaptation of feature detectors. arXiv arXiv:1207.0580, 2012.
29. Watkins, J.C. Probability Theory. In Course Note for Probability Theory, University of Arizona: Tucson, AZ, USA, 2006.
30. Jia, Y.; Shelhamer, E.; Donahue, J.; Karayev, S.; Long, J.; Girshick, R.; Guadarrama, S.; Darrell T.Caffe Convolutional architecture for fast feature embedding. In Proceedings of the ACM International Conference on Multimedia, Orlando, FL, USA, pp.675–678, 2014. https://doi.org/10.1145/2647868.2654889
31. Lei Wang, K. Andrea Scott et al., Sea Ice Concentration Estimation during Freeze-Up from SAR Imagery Using a Convolutional Neural Network, 2017. https://doi.org/10.3390/rs9050408
32. Jessica L. Matthews et al. Sensitivity of Arctic Sea Ice Extent to Sea Ice Concentration Threshold Choice and Its Implication to Ice Coverage Decadal Trends and Statistical Projection, 2014.
33. R. Lindsay and D. Rothrock et al., The calculation of surface temperature and albedo of Arctic sea ice from AVHRR, December 2012.
34. Qing Ji, et al., Statistical Analysis of SSMIS Sea Ice Concentration Threshold at the Arctic Sea Ice Edge during Summer Based on MODIS and Ship-Based Observational Data. Sensors.
35. Venkata KondaReddy Gajjala et al.," AN EFFICIENT MULTI-CLASS SUPPORT VECTOR MACHINE CLASSIFICATION OF AMSR-E DATASET IMAGES, ISSN: 2096-3246, Volume 54, Issue 02, October 2022.
36. Venkata KondaReddy Gajjala et al.," AN EFFICIENT K-NEAREST NEIGHBOR CLASSIFICATION OF AMSR-E DATASET IMAGES", ISSN: 2096-3246, Volume 54, Issue 02, October 2022.

AUTHOR'S PROFILE

Dr. Venkata Konda Reddy Gajjala received a B.Tech Degree in Computer Science and Information Technology, M.Tech in Software Engineering at Jawaharlal Technological University, Hyderabad in 2005, 2010, respectively and completed Ph.D in Image Processing from the Department of CSE, Saveetha Institute of Medical and Technical Sciences in 2024, Chennai. He had more than 16 Years of experience in teaching. He has published five research papers in various international and national journals and Conferences. His areas of interest include image processing, Wireless Communication, Machine Learning, Deep Learning, and AI.

Dr. T. J. Naga Lakshmi obtained her Bachelor's degree in Electronics and Communication Engineering from the University of Madras in 2003 and her Master's degree in Applied Electronics from Anna University, India, in 2007. Completed her Ph.D in 2019 in Electronics Engineering from Saveetha Institute of Medical and Technical Sciences, India. Currently, she has over 20 years of experience in academic teaching and more than 1 year of experience in Research. She has published more than 75 articles in IEEE conferences and Scopus/SCIE Journals. Her areas of interest include image processing, Wireless Communication, Machine Learning, Deep Learning, and VLSI Design. She is a member of the IET and IAENG.